# Monophasic TiO 2 films deposited on SrTiO 3 (100) by pulsed laser ablation

C. C. Hsieh, K. H. Wu, J. Y. Juang, T. M. Uen, J.-Y. Lin, and Y. S. Gou

Citation: Journal of Applied Physics **92**, 2518 (2002); doi: 10.1063/1.1499522
View online: http://dx.doi.org/10.1063/1.1499522
View Table of Contents: http://scitation.aip.org/content/aip/journal/jap/92/5?ver=pdfcov
Published by the AIP Publishing

# Monophasic $TiO_2$ films deposited on $SrTiO_3(100)$ by pulsed laser ablation

C. C. Hsieh,[a] K. H. Wu, J. Y. Juang, and T. M. Uen
*Department of Electrophysics, National Chiao Tung University, Hsinchu 300, Taiwan, Republic of China*

J.-Y. Lin
*Institute of Physics, National Chiao Tung University, Hsinchu, Taiwan 300, Republic of China*

Y. S. Gou
*Department of Electrophysics, National Chiao Tung University, Hsinchu 300, Taiwan, Republic of China*

(Received 5 April 2002; accepted for publication 17 June 2002)

Single phase $TiO_2$ thin films, of either rutile or anatase structure, have been prepared on $SrTiO_3$(STO)(100) substrates by *in situ* pulsed laser deposition (PLD). Thermodynamically unfavorable, for films deposited on STO(100) substrate directly, pure anatase $TiO_2$(00l) films were formed even when a rutile $TiO_2$(110) substrate was used as a target. On the other hand, pure rutile $TiO_2$(110) films were obtained by oxidizing PLD TiN films *in-situ* at temperatures higher than 700 °C. The optimized deposition conditions for preparing TiN and $TiO_2$ films were reported. The crystalline structure, surface morphology, and electronic structure of these films were examined. A mechanism of the process of film formation is also proposed. © *2002 American Institute of Physics.* [DOI: 10.1063/1.1499522]

## I. INTRODUCTION

Titanium dioxide ($TiO_2$) thin films have been studied and used extensively[1–6] since it possesses many unusual properties such as excellent optical transmittance (>85%) in visible and near infrared wavelength, high index of refraction ($n=2.35$ at 550 nm), high chemical stability, and mechanical durability. The widespread applications of $TiO_2$ films include: (a) antireflecting and protective coating on optical elements, (b) capacitors or gates in microelectronic devices, (c) gas and humidity sensors, and (d) optical waveguide in integrated optics. Recently, it has been found that, due to its large dielectric constant ($\varepsilon_r=105$ at 4.2 K) and low tangential loss ($\tan\delta=10^{-7}$ at 4.2 K),[7,8] $TiO_2$ might be an important material in depositing high $T_c$ superconducting $YBa_2Cu_3O_7$ (YBCO) films for microwave applications. Moreover, since YBCO(001) can grow on $TiO_2$-templated Sr $TiO_3$ (STO)(110) substrate, it is possible to grow YBCO(103)/YBCO(001) biepitaxial junctions on a STO(110) substrate. Research toward this direction is in progress. Finally, it is also a good buffer layer for obtaining high quality $CrO_2$[9] and $LaSrMnO_3$[10] films, which might be of vital importance for emerging spintronics application.[11]

Crystalline $TiO_2$ exists in three phases: anatase, rutile, and brookite. Single phase $TiO_2$ thin films with well controlled orientation and smooth surface morphology are essential for studying the properties of respective phases and for practical applications. According to the phase diagram of $TiO_2$,[12] the rutile phase is thermodynamically preferred at high temperature and it is expected that no pure anatase phase can exist at temperatures higher than 650 °C. However, epitaxial growth of pure anatase $TiO_2$ films is highly desirable because the anatase form has been shown to have higher photocatalytic activity than rutile for certain reaction.[13–14] Chen *et al.*[15] have used the metalorganic chemical vapor deposition technique to prepare monophasic anatase and rutile films on STO and sapphire substrates, respectively. They showed that the pure anatase phase can be grown on STO(100) even when the substrate temperature $T_s$ was higher than 900 °C. This indicates that substrate structure can play a significant role in controlling the heteroepitaxial growth of $TiO_2$ films.

The deposition of $TiO_2$ thin films by pulsed laser deposition (PLD) has been reported previously.[16–18] The structural properties, crystallinity, and the surface morphology of the $TiO_2$ films deposited on Si, MgO, and sapphire substrates under various deposition conditions such as oxygen partial pressure $P_{O_2}$ and substrate temperature were investigated. Generally speaking, the structure of the obtained films is strongly dependent on the substrate used, substrate temperature, and the gas pressure. In this article, we shall first describe the optimized conditions for obtaining single phase anatase and rutile $TiO_2$ films deposited on STO(100) substrate by PLD. The crystalline structure, surface morphology and electronic structure of these films, which were examined by x-ray diffraction (XRD), atomic force microscopy (AFM), and x-ray absorption spectroscopy (XAS), respectively, will be presented. The phase formation mechanisms for each process are also elucidated.

## II. EXPERIMENTAL DETAILS

The PLD system used for preparing the TiN and $TiO_2$ films is the same as that reported previously.[19] Briefly, a KrF excimer laser operating at a repetition rate of 3–8 Hz with an

[a]Author to whom correspondence should be addressed; electronic mail: cchsieh.ep90g@nctu.edu.tw

 

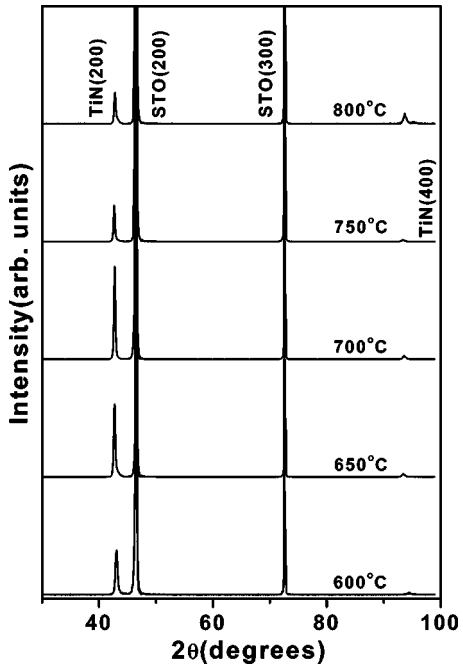


FIG. 1. The XRD patterns of the TiN films deposited at various $T_s$: 600, 650, 700, 750°C, and 800 °C. The pressure was kept at background pressure ($5\times10^{-6}$ Torr).

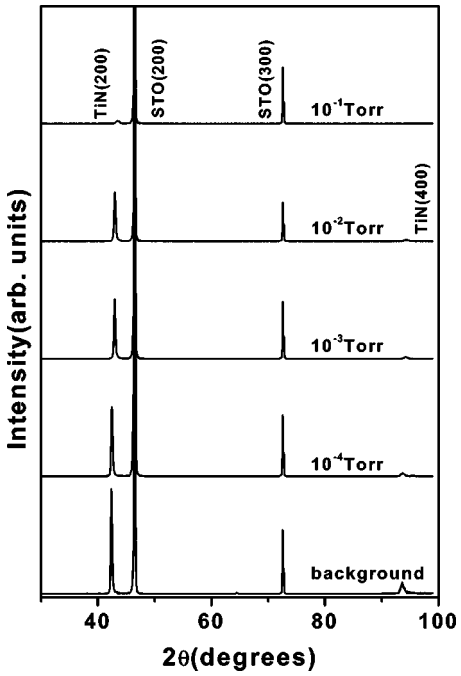


FIG. 2. The XRD patterns of the TiN films deposited at various $P_{N_2}$: background pressure ($5\times10^{-6}$ Torr), $10^{-4}$, $10^{-3}$, $10^{-2}$, and $10^{-1}$ Torr. The $T_s$ was kept at 800 °C.

energy density of 2–5 J/cm$^2$ was used. The target for preparing TiN films was a hot-pressed TiN (99.9%, purity) pellet while that for preparing anatase $TiO_2$ films was a 10-mm-diam rutile $TiO_2$(110) single crystal. The $T_s$ was monitored by a thermocouple attached to the substrate holder. The system was operated in the temperature range of 25–1000 °C and the nitrogen (oxygen) partial pressures range of background pressure ($5\times10^{-6}$ Torr at 780 °C) to 0.5 Torr to optimize the deposition conditions for various films investigated in this study.

The crystalline structure of the films was examined by XRD (Rigaku D/max-rc/ru200b), using Cu $K\alpha$ radiation. The surface morphology of the films was investigated by means of AFM (Digital Instruments DI 5000), and scanning electron microscopy. The electronic structure of the $TiO_2$ films was examined by XAS, using the 6 m high-energy spherical monochromatic (HSGM) beam line at Synchrotron Radiation Research Center (SRRC), Taiwan, Republic of China.[20]

## III. RESULTS AND DISCUSSION

### A. Preparation of rutile $TiO_2$ thin films

To prepare the rutile $TiO_2$ films, TiN films were deposited on the STO(100) substrate at first, using a laser energy density of 5 J/cm$^2$ and a repetition rate of 5 Hz. The deposition rate under these conditions was about 0.02 nm/pulse. The blue plume could be easily observed during ablation. The $T_s$ was varied from 600 to 800 °C and the nitrogen partial pressures $P_{N_2}$ was varied from background pressure ($5\times10^{-6}$ Torr at 700 °C) to 0.1 Torr. Figure 1 shows the XRD patterns of the TiN films deposited at various $T_s$ while keeping the pressure at background pressure. Figure 2 shows the XRD patterns of the TiN films deposited at various $P_{N_2}$ while keeping $T_s$ at 700 °C. The best TiN films (consider the crystallinity) were obtained under the background pressure and at $T_s=700$ °C. The resistivity versus temperature curve, XRD pattern, and AFM image of a typical PLD TiN film deposited at the optimized conditions were shown in Figs. 3(a)–3(c), respectively. The as-deposited film was about 60 nm thick and was shiny golden yellow in appearance. The resistivity of the film [Fig. 3(a)] was less than $2\mu\Omega$ cm at 77 K. The nearly perfect metallic behavior and the diminishingly small residual resistance below 20 K are indicative of almost impurity-free crystallinity. The full width at half maximum (FWHM) of the $\theta$–$2\theta$ diffraction peak for TiN(200) was about 0.18° [Fig. 3(b)]. The surface morphology as revealed by AFM [Fig. 3(c)], shows an average grain size of about 50 nm with an atomically smooth surface. The root mean square (rms) roughness of the surface was estimated to be about 0.2 nm.

The PLD TiN films were then *in situ* oxidized at various $T_s$ ranging from 500 to 900 °C for 60 min. The oxygen partial pressure for the oxidation process was 5 Torr. Figure 4(a) shows the XRD results for films annealed at different temperatures. For $T_s$ at (and below) 500 °C, the TiN(200) peak persisted and no $TiO_2$ peak was found. This implies that the oxidation rate is too slow under the oxidation condition to convert TiN film into $TiO_2$.[21] For $T_s=600$ °C, the TiN(200) peak disappeared but no apparent diffraction peak corresponding to $TiO_2$ was found. The $TiO_2$ films formed at this temperature might be amorphous. The pure rutile (110) peak appeared when $T_s$ was raised up to 700 °C. The intensity of the peak increased and the FWHM of the peak decreased with increasing $T_s$. Figure 5(a) shows a typical AFM image of TiN films oxidized at 800 °C. The grain size of the rutile $TiO_2$ thus obtained is about 400 nm, which is much larger

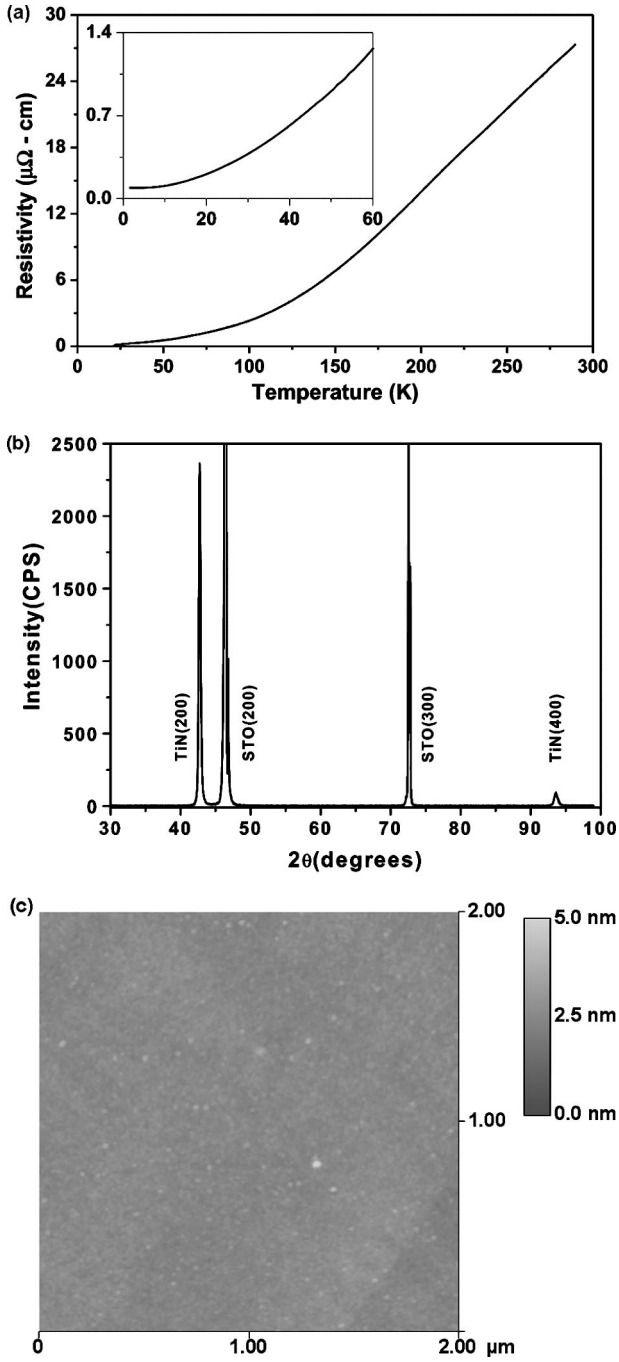


FIG. 3. (a) The resistivity vs temperature curve, (b) the XRD pattern, and (c) the AFM image of the TiN(100) film deposited on STO(100) substrate. The PLD deposition conditions were $T_s = 700\,^{\circ}\mathrm{C}$ and at background pressure. The scanned area of the AFM image was 2 $\mu$m×2 $\mu$m and the dark-to-light vertical scale was 5 nm.

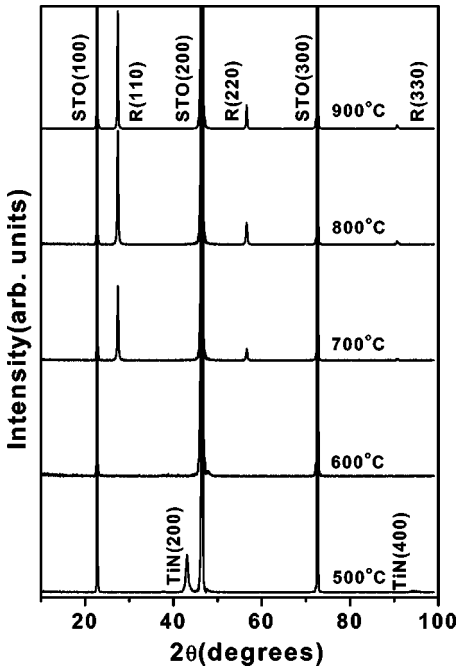


FIG. 4. The XRD patterns of the PLD TiN films oxidized at various $T_s$: 500, 600, 700, 800, and 900 °C. The oxidation time was 60 min and the $P_{O_2}$ was kept at 5 Torr. (*R*: rutile $TiO_2$, *A*:anatase $TiO_2$).

than that of the original TiN films. A greater variation in roughness (rms roughness ~0.8 nm) can also be observed in the figure. The change of surface roughness may have resulted from the large volume expansion during oxidation.

### B. Preparation of anatase $TiO_2$ thin films

In order to reduce particulates landing during PLD, a 10-mm-diam rutile $TiO_2(110)$ single crystal substrate was used as the target. The laser parameters for depositing $TiO_2$ films were the same as those for depositing TiN films. The $T_s$ was varied from 25 to 1000 °C (limited by heater) and the $P_{O_2}$ was varied from background pressure ($5\times10^{-6}$) to 0.1 Torr. The deposition rate was about 0.05 nm/pulse.

Figure 6 shows the $T_s$ dependence of XRD patterns of the $TiO_2$ films at $P_{O_2} = 0.01$ Torr. Figure 7 shows the $P_{O_2}$ dependence of XRD patterns of the films at $T_s = 800\,^{\circ}\mathrm{C}$. It was found that when the $TiO_2$ films was deposited on STO(100) by direct ablation of the $TiO_2$ target, the anatase phase was formed over a wide range of deposition parameters. Pure anatase $TiO_2$ films were obtained for $T_s$ ranging from 200 to 1000 °C and $P_{O_2}$ ranging from background ($5\times10^{-6}$) to 0.1 Torr. However, the best films were obtained at $T_s = 800\,^{\circ}\mathrm{C}$ and $P_{O_2} = 10^{-2}$ Torr. Figure 5(b) shows the AFM image of an 60-nm-thick $TiO_2$ thin film deposited at the above-mentioned conditions. The surface morphology shows an average grain size of about 50 nm. The rms roughness of the surface was about 0.25 nm. It seems that, although the phase is different, the surface is very smooth for both PLD TiN transferred $TiO_2$ and PLD $TiO_2$ films.

As an independent check, both forms of $TiO_2$ films were further examined by means of XAS measurements. The XAS experiments on the O *1s* and Ti *2p* spectra were performed on the 6 m HSGM beam line at the SRRC.[19] The spectra were recorded in both total-electron yield (TEY) mode and x-ray-fluorescence yield mode, which revealed the surface and bulk properties, respectively.[22] Figures 8(a)–8(e) and 9(a)–9(e) show the O *1s* and Ti *2p* spectra for (a) standard rutile $TiO_2$ powder, (b) rutile $TiO_2(110)$ substrate, (c) $TiO_2$ films transformed from PLD TiN films, (d) standard anatase $TiO_2$ powder, and (e) direct PLD $TiO_2$ films, respectively. The position and intensity of the peaks in the spectra have been

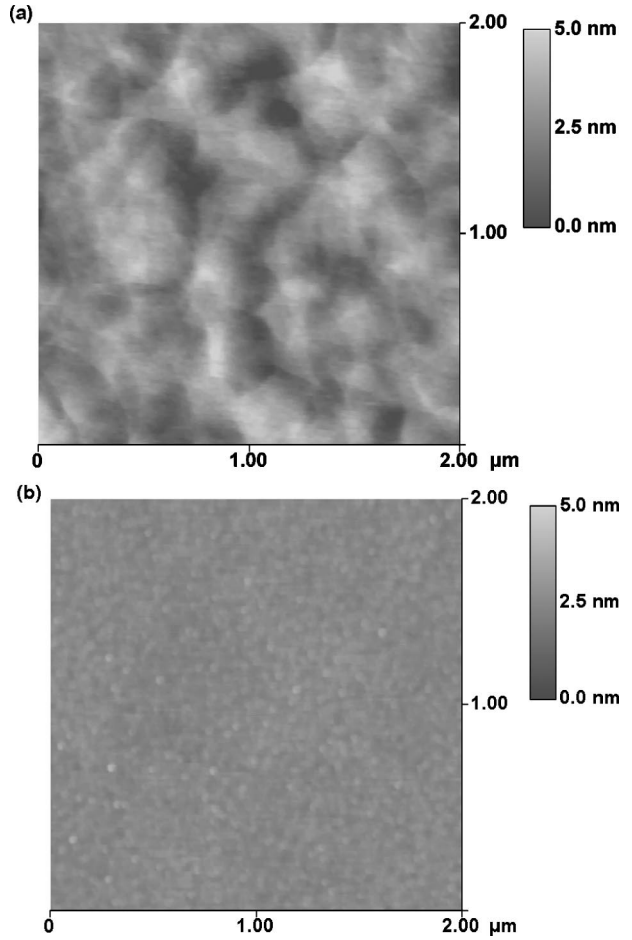


FIG. 5. (a) The AFM image of the rutile $TiO_2(110)$ films oxidized from PLD TiN films. The $T_s$ was kept at 780 °C and $P_{O_2}$ was kept at 5 Torr. (b) The AFM image of the anatase $TiO_2(001)$ films prepared by PLD directly. The $T_s$ was kept at 800 °C and $P_{O_2}$ was kept at 0.01 Torr. All the images are 2 $\mu$m×2 $\mu$m and the dark-to-light vertical scale is 5 nm.

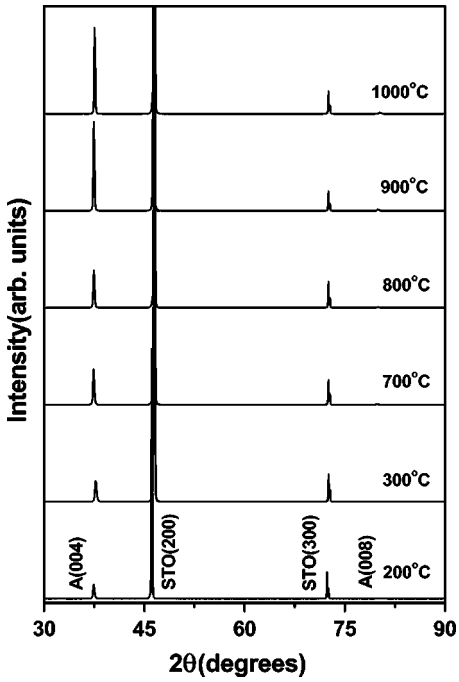


FIG. 6. The XRD patterns of the PLD $TiO_2$ films deposited at various $T_s$: 200, 300, 700, 800, 900, and 1000 °C. The $P_{O_2}$ was kept at 0.01 Torr. (*R*:rutile $TiO_2$, *A*:anatase $TiO_2$).

calculated and assigned in.[23–26] For the O *1s* spectra, it can be roughly divided into two regions. The first region covers the energy range 530–537 eV and is attributed to the O *2p* state hybridized to Ti *3d* states. The Ti *3d* region is split by a crystal field effect and is characterized as a doublet. The second region, above 537 eV, is attributed to the O *2p* states hybridized to Ti *4sp* bands. As shown in Fig. 8, although the peaks lying in the first region have no significant difference between rutile and anatase, there does exist differences in the peaks lying in the second region. At this higher energy region, rutile exhibits three peaks *C*1, *C*2, and *C*3 while anatase shows only two peaks *C*1 and *C*2. On the other hand, the significant difference in the Ti *2p spectra* (Fig. 9) for rutile and anatase is the relative intensity of peaks *P*1 and *P*2. The intensity of peak *P*1 is higher than that of peak *P*2 for rutile while the opposite trend is true for anatase.[23,26] The obtained intensity variations of these spectra are consistent with those measured by Brydson *et al.*[26] and de Groot *et al.*[27–29] and evidently indicate that the $TiO_2$ films are indeed pure anatase or rutile phase.

### C. Discussion

From the above results, it is clear that either pure anatase or pure rutile $TiO_2$ films have been evidently obtained on the STO(100) substrate. As mentioned in Sec. I, without taking the substrate effect into account, rutile is the thermodynamically stable phase of $TiO_2$ at temperatures higher than 650 °C and should be the predominant phase above this temperature. However, for the case of $TiO_2$ films deposited on STO(100) directly, anatase $TiO_2$ was formed even when $T_s = 1000$ °C.

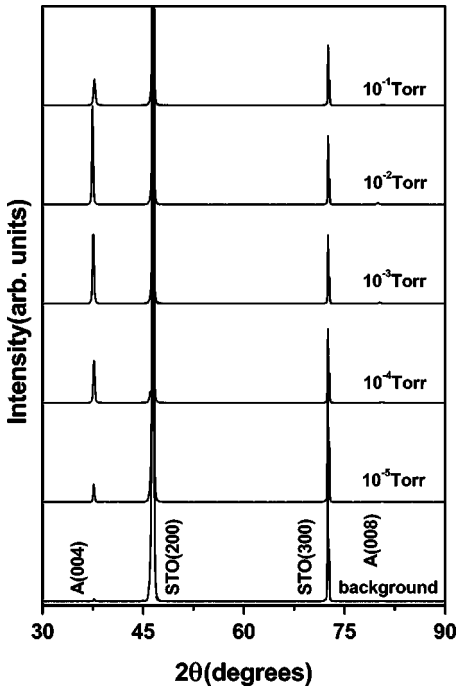


FIG. 7. The XRD patterns of the PLD $TiO_2$ films deposited at various $P_{O_2}$: background pressure ($5\times10^{-6}$ Torr), $10^{-5}$, $10^{-4}$, $10^{-3}$, $10^{-2}$, and $10^{-1}$ Torr. The $T_s$ was kept at 800 °C. (*R*:rutile $TiO_2$, *A*:anatase $TiO_2$).

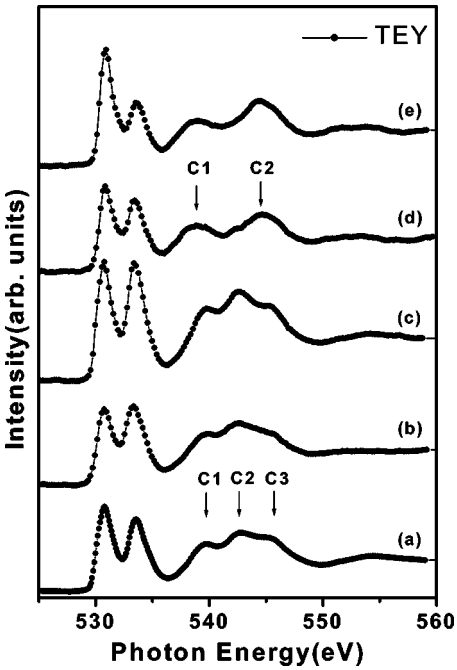


FIG. 8. The XAS spectra of the O *1s spectra for*: (*a*) *standard rutile* $TiO_2$ *powder*, (*b*) *rutile* $TiO_2(110)$ *substrate* (*used as a target for PLD* $TiO_2$ *films*), (*c*) $TiO_2$ *films transformed from PLD TiN films*, (*d*) *standard anatase* $TiO_2$ *powder, and* (*e*) *direct PLD* $TiO_2$ *films. The TEY mode is plotted as a solid line.*

It suggests that anatase may be kinetically stable under this deposition condition. This additional stability can be understood by examining the lattice constants and (001) planar structures of the STO and anatase $TiO_2$. Figure 10 shows the crystallographic structures of STO and $TiO_2$. As shown in

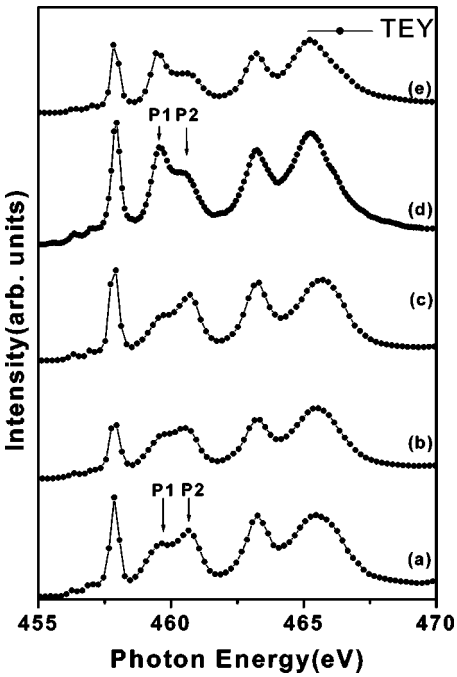


FIG. 9. The XAS spectra of the Ti *2p* spectra for (a) standard rutile $TiO_2$ powder, (b) rutile $TiO_2(110)$ substrate (used as a target for PLD $TiO_2$ films), (c) $TiO_2$ films transformed from PLD TiN films, (d) standard anatase $TiO_2$ powder, and (e) direct PLD $TiO_2$ films.

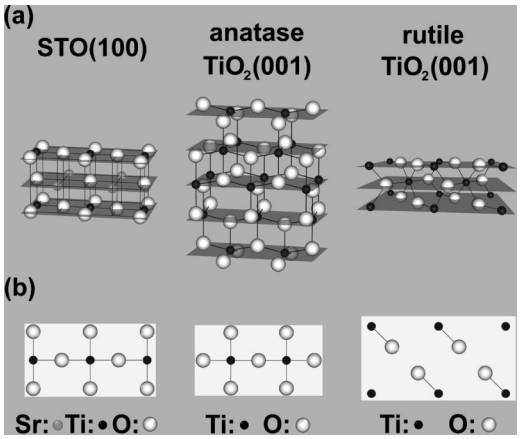


FIG. 10. (a) The three-dimensional view of the crystallographic structures of STO(100), anatase $TiO_2(001)$, and rutile $TiO_2(001)$. (b) The (001) planar structure of STO, anatase $TiO_2$, and rutile TiO2.

Fig. 10(a), STO is cubic with $a=b=c=3.904$ Å, while anatase and rutile $TiO_2$ are tetragonal with $a=b=3.785$ Å, $c=9.515$ Å for anatase; and $a=b=4.593$ Å, $c=2.959$ Å for rutile, respectively. The in-plane lattice mismatch between STO(100) and anatase $TiO_2$ is ~3% while that between STO(100) and rutile $TiO_2$ is ~15%. Moreover, by comparing the planar atomic configuration among STO(100), anatase $TiO_2(001)$, and rutile $TiO_2(001)$ planes [Fig. 10(b)], it is clear that the similarities exhibited between the STO(100) and anatase $TiO_2(001)$ may also play an important role. In this scenario one expects that during the initial stage of film growth the arriving Ti and O atoms will tend to align themselves with the existing Ti and oxygen sublattices of the STO substrate. This process naturally leads to the formation of (001) anatase phase despite that it is not a thermodynamically favorable phase. It is remarkable that the anatase $TiO_2(001)$ film can be stabilized by STO(100) substrate and sustained to such high temperatures.

Now let us consider the case of the oxidation of PLD TiN films. Since the oxidation proceeds into the bulk from the surface, this process is expected to have much weaker relevance to the effect of substrate. Therefore, the rutile $TiO_2$ phase is the preferred phase when the TiN is oxidized at temperatures higher than 650 °C. If we further compare the crystallographic structure of TiN (001) and rutile $TiO_2(110)$ (as depicted in Fig. 11), we found that the relative configuration of Ti atoms remains almost intact with only a slight change in interatomic distance. Since a much higher activation energy is required for moving the Ti atoms,[28] the oxidation ought to proceed by keeping Ti atoms remaining in the vicinity of their original location while the migration and desorption of N atoms and the intake of O atoms and formation of rutile Ti–O bonding take place. In this scenario, rutile $TiO_2(110)$ is the most preferred phase and orientation for the oxidation of TiN(100) films.

## IV. SUMMARY

Two phases of $TiO_2$ thin films—rutile and anatase—have been prepared on $SrTiO_3$(STO)(100) substrates by *in situ* PLD. The anatase phase was prepared by pulsed ablation

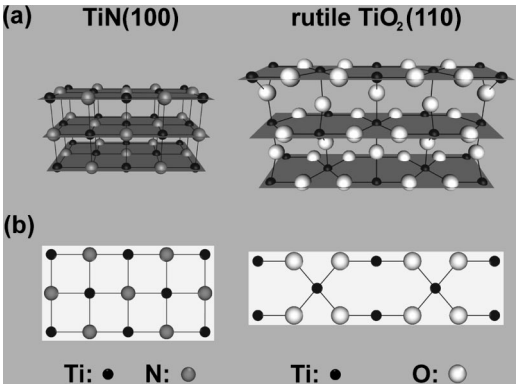


FIG. 11. (a) The three-dimensional view of the crystallographic structures of TiN(100) and rutile $TiO_2$(110). (b) The planar structure of TiN(100) and rutile $TiO_2$(110).

of the $TiO_2$ target directly while the rutile phase was prepared by PLD of TiN film and then oxidized it *in situ* in the vacuum chamber. The formation of anatase $TiO_2$(00l) films on the STO(100) substrate at temperatures up to 1000 °C indicates that the structure and orientation of the substrate may have played an important role in controlling the phase and orientation of the deposited films. On the other hand, since the oxidation starts from the surface of TiN films, rutile $TiO_2$ is preferred to form when the TiN was oxidized at temperatures higher than 700 °C. The similar configuration of the Ti atoms on the TiN(001) plane and rutile $TiO_2$(110) plane explains the preferred orientation of $TiO_2$(110) observed in the present study.

## ACKNOWLEDGMENT

This work was supported by the National Science Council of Taiwan, Republic of China under Grant Nos. NSC90-2112-M-009-036.

[1] B. Weinberger and R. Garber, Appl. Phys. Lett. **66**, 2409 (1995).
[2] K. Vorotilov, E. Orlova, and V. Petrovsky, Thin Solid Films **207**, 180 (1992).
[3] W. D. Brown and W. W. Grannemann, Solid-State Electron. **21**, 837 (1978).
[4] K. M. Glassford and J. R. Chelikowsky, Phys. Rev. B **46**, 1284 (1992).
[5] A. Perry and K. Pulker, Thin Solid Films **124**, 323 (1985).
[6] S. A. Chambers, Surf. Sci. Rep. **39**, 105 (2000).
[7] N. J. Parker, P. Kharel, J. R. Powell, P. A. Smith, P. D. Evans, and A. Porch, IEEE Trans. Appl. Supercond. **9**, 1928 (1999).
[8] C. Zuccaro, I. Ghosh, K. Urban, N. Klein, S. Penn, and N. M. Alford, IEEE Trans. Appl. Supercond. **7**, 3715 (1997).
[9] S. J. Liu, J. Y. Lin, J. Y. Juang, K. H. Wu, T. M. Uen, and Y. S. Gou, Appl. Phys. Lett. **80**, 4202 (2002).
[10] S. J. Liu, J. Y. Lin, J. Y. Juang, K. H. Wu. T. M. Uen, and Y. S. Gou, Appl. Phys. Lett. (submitted).
[11] S. T. Bramwell and M. J. P. Gingras, Science **294**, 1495 (2001).
[12] F. Dachille, P. Y. Simons, and R. Roy, Am. Mineral. **53**, 1929 (1968).
[13] L. Kavan, M. Gratzel, S. E. Gilbert, C. Klemens, and H. J. Scheel, J. Am. Chem. Soc. **118**, 6716 (1996).
[14] H. Tang, K. Prasad, R. Sanjinés, P. E. Schmid, and F. Lévy, J. Appl. Phys. **75**, 2042 (1994).
[15] S. Chen *et al.*, J. Vac. Sci. Technol. A **11**, 2419 (1993).
[16] H. A. Durand, J. H. Brimaud, O. Hellman, H. Shibata, Y. Makita, D. Gesbert, and P. Meyrueis, Appl. Surf. Sci. **86**, 122 (1995).
[17] C. Garapon, C. Champeaux, J. Mugnier, G. Panczer, P. Marchet, A. Catherijot, and B. Jacquier, Appl. Surf. Sci. **96–98**, 836 (1996).
[18] J. H. Kim, S. Lee, and H. S. Im, Appl. Surf. Sci. **151**, 6 (1999).
[19] K. H. Wu, J. Y. Juang, C. L. Lee, T. C. Lai, T. M. Uen, Y. S. Gou, S. L. Tu, S. J. Yang, and S. E. Hsu, Physica C **195**, 241 (1992).
[20] S. C. Chung *et al.*, Rev. Sci. Instrum. **66**, 1655 (1995).
[21] M. Wittmer, J. Noser, and H. Melchior, J. Appl. Phys. **52**, 6659 (1981).
[22] J. Stohr, *NEXASFS Spectroscopy*, Springer Series in Surface Sciences, Vol. 25 (Springer, Berlin, 1992).
[23] D. W. Fischer, Phys. Rev. B **5**, 4219 (1972).
[24] J. Pflüger, J. Fink, W. Weber, K. P. Bohnen, and H. Winter, Solid State Commun. **44**, 489 (1982).
[25] L. Soriano, M. Abbate, J. C. Fuggle, P. Prieto, C. Jiménez, J. M. Sanz, L. Galán, and S. Hofmann, J. Vac. Sci. Technol. A **11**, 47 (1993).
[26] R. Brydson, H. Sauer, W. Engel, J. M. Thomas, E. Zeitler, N. Kosugi, and H. Kuroda, J. Phys.: Condens. Matter **1**, 797 (1989).
[27] F. M. F. de Groot, M. Grioni, J. C. Fuggle, J. Ghijsen, G. A. Sawatsky, and H. Petersen, Phys. Rev. B **40**, 5715 (1989).
[28] F. M. F. de Groot, J. C. Fuggle, B. T. Thole, and G. A. Sawatsky, Phys. Rev. B **41**, 928 (1990).
[29] F. M. F. de Groot, J. Faber , J. J. M. Michiels, M. T. Czyżyk, M. Abbate, and J. C. Fuggle, Phys. Rev. B **48**, 2074 (1993).